



Open your mind. LUT.
Lappeenranta University of Technology

Faculty of Technology

Laboratory of Steel Structures

Lappeenranta University of Technology

Charles Addai

Capacity of an I-beam made of S960 QC based on Eurocode 3

Examiners: Professor Timo Björk

Dr (Tech) Tapani Halme

ABSTRACT

Author: Charles Addai
Title: Capacity of an I-beam made of S960 QC based on Eurocode 3.
Year: 2013
Master's Thesis: Thesis for the Degree of Masters of Science in Technology
65 pages, 16 figures, 10 tables, 5 appendices.
Examiners: Prof. Timo Bjork
Dr (Tech) Tapani Halme
Keywords: throat thickness, elastic capacity, moment, buckling, fatigue life.

The capacity of beams is a very important factor in the study of durability of structures and structural members. The capacity of a high-strength steel I-beam made of S960 QC was investigated in this study. The investigation included assessment of the service limits and ultimate limits of the steel beam. The thesis was done according to European standards for steel structures, Eurocode 3. An analytical method was used to determine the throat thickness, deformation, elastic and plastic moment capacities as well as the fatigue life of the beam. The results of the analytical method were compared with those obtained by Finite Element Analysis (FEA).

Elastic moment capacity obtained by the analytical method was 172 kNm. FEA and the analytical method predicted the maximum lateral-torsional buckling (LTB) capacity in the range of 90-93 kNm and the probability of failure as a result of LTB is estimated to be 50%. The lateral buckling capacity meant that the I-beam can carry a safe load of 300 kN instead of the initial load of 600 kN. The beam is liable to fail shortly after exceeding the elastic moment capacity. Based on results in of the different approaches, it was noted that FEA predicted higher deformation values on the load-deformation curve than the analytical results. However, both FEA and the analytical methods predicted identical results for nominal stress range and moment capacities. Fatigue life was estimated to be in the range of 53000-64000 cycles for bending stress range using crack propagation equation and strength-life approach. As Eurocode 3 is limited to steel grades up to S690, results for S960 must be verified with experimental data and appropriate design rules.

ACKNOWLEDGEMENTS

This thesis would be incomplete without expressing my great appreciation to Prof. Timo Björk for providing such an interesting thesis topic. Prof. Björk's care and guidance was of great help in completion of this thesis project.

Appreciation goes to Dr (Tech) Tapani Halme for teaching me the basics of strength of materials and FE-analysis and directing my interest towards analysis of steel I-beams.

Tuomas Laamanen, a co-researcher, is acknowledged for his contributions and the initial design of the I-beam profile.

Lastly, the author is grateful to all friends and loved ones for their support and encouragement. To Eeva-Liisa, Peter Jones, Simon and Kwadwo I say thank you!

Table of Content

ABSTRACT	i
AKNOWLEDGEMENTS	ii
Table of Content.....	iii
List of Symbols and Abbreviations.....	v
List of Figures	viii
List of Tables.....	ix
1. INTRODUCTION	1
1.1 Background	1
1.2 Scope and Limitations.....	2
1.3 Aim of the Thesis:.....	3
2. MATERIALS AND METHODS	4
2.1 S960 QC	4
2.2 Analytical Methods	5
2.3 Cross Section Properties, Formulas and Numerical Values.....	6
2.3.1 I-Beam Profile.....	6
2.3.2 Throat Thickness	8
2.3.3 Local Buckling Check.....	10
2.3.4 Effective Cross Section Properties.....	12
3 FAILURE CRITERIA	20
3.1 General Failure Criteria.....	20
3.2 Deflection	20
3.3 Elastic Limit	21
3.4 Stability	23
3.5 Capacities of I-Beam.....	25


3.5.1 Buckling Capacity	25
3.5.2 Plasticity	31
3.6 Fatigue Strength	33
3.7 Brittle Fracture	40
4 COMPARISON WITH FEA RESULTS	42
5 CONCLUSIONS	45
REFERENCES	47
APPENDICES	52
Appendix 1 Stress distributions for effective width (1993-1-5:2006, p.17)	
Appendix 2 Buckling curves (SFS EN 1993-1-1:2005(E), p.59)	
Appendix 3 Fatigue strength curves for direct stress ranges (EN 1993-1-9: 2005(E), p. 15)	
Appendix 4 Fatigue strength curves for shear stress ranges (EN 1993-1-9: 2005(E), p. 16)	
Appendix 5 Inputs and function for fatigue life calculation based on Paris equation	

List of Symbols and Abbreviations

Eurocode 3 symbols:

A	area
A_{eff}	effective cross sectional area
$A_{c,eff}$	effective plate area of members under compression
A_{ft}	area of tension flange
A_w	area of web
A_5	minimum elongation
a	throat thickness
b, b_f	width of flange
b_{eff}	effective plate width
c	centroid
E	modulus of elasticity
f_y	yield stress
G	shear modulus
h_w	web height between flanges
I	moment of inertia of the cross section
I_t	torsional constant
I_w	warping constant
I_z	second moment of area about the weak axis
K_{IC}	fracture toughness in mode I loading

l, L	length, effective length
M_{cr}	elastic critical moment for lateral-torsional buckling
$M_{b,Rd}$	design buckling resistance moment
M_{Ed}	design value of bending moment
$N, \Delta N$	fatigue life, endurance, number of cycles
N_R	designed life time expressed as number of cycles related to a constant stress range
P	load
S	first moment of area about centroidal axis
t	thickness of the plate
V_{Ed}	design value of shear force
W_y, W_{el}	elastic section modulus
Z	plastic section modulus
β_w	fillet weld correction factor
δ	deflection, deformation,
σ_{max}	maximum stress
$\Delta\sigma$	stress range
σ_y	yield stress
$\Delta\tau$	stress range (shear stress)
$\Delta\sigma_c$	reference value of fatigue strength at $N_c = 2$ million cycles

$\Delta\sigma_D$	fatigue limit for constant amplitude stress ranges at the number of cycles
$\Delta\sigma_L$	cut-off limit for stress ranges at the number of cycles N_L
λ_{LT}	non-dimensional slenderness for lateral-torsional buckling
	fillet weld

Abbreviations:

LTB lateral torsional buckling

NA neutral axis

KV charvy impact energy

HAZ heat affected zone

List of Figures

Figure 1 Side views of the I-beam (Laamanen, 2013).....	7
Figure 2 Throat thickness of a fillet weld based on EN 1993-1-8.	8
Figure 3 Effective plate areas.....	13
Figure 4 Computation of plastic section modulus for doubly symmetric I-beam.....	17
Figure 5 I- beam parameters and numerical dimensions.	18
Figure 6 Loading of the I-beam.	21
Figure 7 Stress distribution diagram at the elastic limit.....	22
Figure 8 Lateral buckling of unrestrained I-beam (Punmia, Ashok & Arun, 1998, p.243)	25
Figure 9 Lateral torsional buckling of an unrestrained beam (Wang, 2002, p.13)	25
Figure 10 Point of application of transverse load.	27
Figure 11 Shear and Moment distribution.	28
Figure 12 Plastic moment distribution (Gorenc, Tinyou & Syam, 2005, p. 268).....	32
Figure 13 Fatigue strength curve for bending stress ranges.....	37
Figure 14 Schematic of fatigue crack growth (SAE, 1988, p.254).....	38
Figure 15 Fatigue crack growth.	39
Figure 16 Load-deformation behaviour (Laamanen, 2013).....	42

List of Tables

Table 1 Chemical composition of S960 QC (Björk, Toivonen & Nykänen, 2010).....	5
Table 2 Mechanical properties of S960 QC (Björk, Toivonen & Nykänen, 2010 & SSAB AB).....	5
Table 3 Eurocode 3 recommendation for checking width-to-thickness ratios.....	10
Table 4 warping and torsional constants.....	19
Table 5 Failure criteria at service limit and ultimate limit.....	20
Table 6 Loading constants and effective length factors (Lehtinen, 2005, p.53).....	27
Table 7 Plastic capacity and shape factor for I-beam.	32
Table 8 Data for fatigue strength curve.....	36
Table 9 Comparison of lateral buckling analysis from FEA and analytical method.	43
Table 10 Comparison of static analysis from FEA and analytical method.....	44

1. INTRODUCTION

1.1 Background

Investigation of beam capacity has become a topic of renewed interest in the scientific community as companies involved in the supply of steel structures look for ways to cut down the weight and cost of structural members while ensuring maximum durability and safety. Various approaches have been used to determine the optimum load that a given cross section can withstand for maximum service life. Eurocode 3 is an example of a design standards which sets out design requirements for safe design.

The I-beam under study is made of ultra-high strength steel (UHSS), S960 QC. S960 QC is a thin UHS structural steel with minimum yield strength of 960MPa and is direct-quenched (DQ) (Ruukki & EN 10025). The use of high strength steels in structural elements is one way to save energy and minimise carbon footprint, particularly in mobile equipment (Björk, Toivonen & Nykänen, 2010).

Avery, Mahendran and Nasir (2000) researched the flexural capacity of hollow flange beams using a finite element model and considered factors that might have significant effect on the load-carrying capacity. Such factors included local buckling, member instability, web distortions, residual stresses and geometric imperfections (Avery, Mahendran & Nasir, 2000). These factors are also addressed in this thesis.

Kim and Kim (1998) conducted topology optimisation of thin-walled beam cross sections and related the material density to the modulus of elasticity. This thesis follows the required slenderness ratio for ultimate limits based on the guidelines of Eurocode 3.

Many papers have been published on the capacity of beams assessed with various analytical procedures but few have been published using the guidelines of Eurocode3 (Kim & Kim, 1998, Avery, Mahendran & Nasir 2000). Although Eurocode 3 is limited to steel grades up to S690, it outlines a standardized procedure for assessing the durability of structures for maximum service life. Currently, ultra-high strength metal manufacturers still rely on Eurocode 3 as the basis for design improvement and a research group have proposed that the current design equations could be extended to

steel grades with nominal yield strength range of 1000 MPa (Halme, Huusko & Marquis, 2010).

The I-beam considered in this work is designed based on Eurocode 3 to support a load of 600 kN. The elastic and plastic moment capacities are determined to establish whether the I-beam may fail under bending loads. Designed shear resistance of the fillet welds was evaluated to define the minimum throat thickness for the I-beam. For steel members subjected to bending stresses, the elastic and plastic load-carrying capacities of the cross section depend on the stability of the flanges and the web (Juhás, 2009). Local buckling and flexural buckling modes are checked in accordance with Eurocode 3. The results of the analytical method are compared with FEA results obtained from Laamanen (2013).

Prior to determination of the beam capacities, effective properties such as area, throat thickness, moment of inertia about the neutral axis, elastic and plastic section moduli are determined.

1.2 Scope and Limitations

The study considers the capacity of a laterally unrestrained I-beam subjected to uniform bending. The beam is loaded on two points and it is simply supported at the ends. The effective cross sectional properties and the capacities of the beam are determined based on Eurocode 3. The capacity of the beam under elastic condition is of primary concern. The beam under investigation is a solid I-beam made from S960 QC with specified cross sectional properties. The total area of the fillet welds is negligible in size compared to the whole area of the I-section, and it is neglected from the effective area of the I-beam. Shear lag, plastic deformation, creeping, vibrations and stress corrosions are not treated. Additionally, column-like buckling behaviour of plates is excluded from the study.

1.3 Aim of the Thesis:

To calculate the lateral buckling capacity and fatigue life of an I-beam made of S960 QC according to Eurocode 3.

2. MATERIALS AND METHODS

2.1 S960 QC

S960 QC is a standardized direct quenched ultra-high strength structural steel which has a minimum yield strength of 960 MPa (Ruukki, SFS EN 10025) and contains all the attributes of steel such as strength, toughness and rigidity (International Association for Bridge and Structural Engineering, IABSE, 2005).

Currently, “constructional steel work of Europe is limited to steel grades of up to S690, higher strength grades are still the domain of construction equipment industry” (IABSE, 2005, p.103). According to IABSE (2005), alloying elements (such as carbon and manganese) coupled with heat treatment increase the strength and toughness of the steel but weldability is decreased. Poor weldability may create welding defects which may increase stress concentrations in the throat area. For high strength steels brittle fracture usually occur in the welds, HAZ or base material as a result of residual and applied stresses. It is therefore important to use efficient welding technologies to join the I-beam parts together.

Kalpakjian (2006) claims that the properties and behaviour of metals and metal-alloys during manufacturing and after manufacturing (service life) depend on the composition, structure, and processing history and the effect of heat treatment. According to Kalpakjian (2006), properties such as strength, hardness, ductility, toughness, and resistance to wear are as a result of the alloying elements. Heat treatment modifies the microstructure of the metal and alters some mechanical properties of the metal.

Generally, in the field of structural engineering, the strength of a material refers to the load carrying capacity. Normally, the concept of material strength is understood by the mechanical properties such as modulus of elasticity, tensile strength, yield strength and creep resistance. The material strength is a combination of several properties such as physical, chemical and thermal properties. In this thesis the material strength means the resistance to bending, deformation, buckling and fatigue failure. The following tables give the chemical and mechanical properties of S960 QC:

Table 1 Chemical composition of S960 QC (Björk, Toivonen & Nykänen, 2010).

	C	Mn	Si	P	S	Ti
nominal (max)	0,11	1,20	0,25	0,02	0,01	0,07
measured	0,080	1,04	0,20	0,012	0,004	0,03

The low carbon content ensures high impact toughness after direct quenching and also improves weldability (Hemmilä, Hirvi & Kömi, 2010). “Suitable bainite / martensite hardenability is achieved by controlling the contents of elements like Cr, Cu, Ni, Mo, Nb, V and B” (Hemmilä, Hirvi & Kömi 2010, p.2).

Table 2 Mechanical properties of S960 QC (Björk, Toivonen & Nykänen, 2010 & SSAB AB).

Material		f_y MPa	f_u MPa	A ₅ %	KV(J)	Typical Hardness
S960	Nominal	960	1000	7	50 (-40°C)	310 – 370
4 ≤ t ≤ 53 (SSAB AB)	Measured	1014	1076	12,5		(SSAB AB)

SFS EN10025 put the ultimate tensile strength f_u of S960 steel to within 980-1150 MPa. The minimum value of ultimate tensile strength is used in defining the throat thickness of the I-beam in subsequent calculations.

2.2 Analytical Methods

Analytical methods employed in this study are mainly linear static analysis and elastic buckling analysis. Formulas which incorporate the cross section properties were used to calculate the parameters needed to determine the I-beam capacities. The effective section properties include the area, moment of inertia and section moduli. The warping and torsional constants of the I-beam were also calculated. The cross section properties are defined by the designed rules of Eurocode 3.

The first part of the study deals with the determination of throat thickness of the fillet welds and effective cross section properties of the I-beam. The second part deals with the determination of the elastic and plastic moment capacities of I-beam. Consequently, the third part focuses on fatigue assessment of the beam. A FAT class of 71MPa is used for non-load carrying attachment and for the compressed and bending members (carrying a transverse load), the stress detail category of 80MPa was used in the fatigue assessment.

2.3 Cross Section Properties, Formulas and Numerical Values.

2.3.1 I-Beam Profile

Figure 1 shows the views and the dimensions on the I-beam. The ends of the beam are restricted from rotational capacity by two rectangular plates to prevent flange induced buckling of the web. There are two loading supports which stiffens the web. The top flange is designed to carry the load and it is called the compression flange and the bottom flange is called the tension flange (SFS EN 1993-1-1). The web is joined to the flanges by fillet welds. The details of the fillet welds are presented clearly in section 2.3.2. The I-beam is simply supported with a span of 1600 mm. The fillet welds carry transverse loads along the ends of the web on both sides. Eurocode 3 gives the provision for transverse stiffeners if the designed resistance of unstiffened web is insufficient.

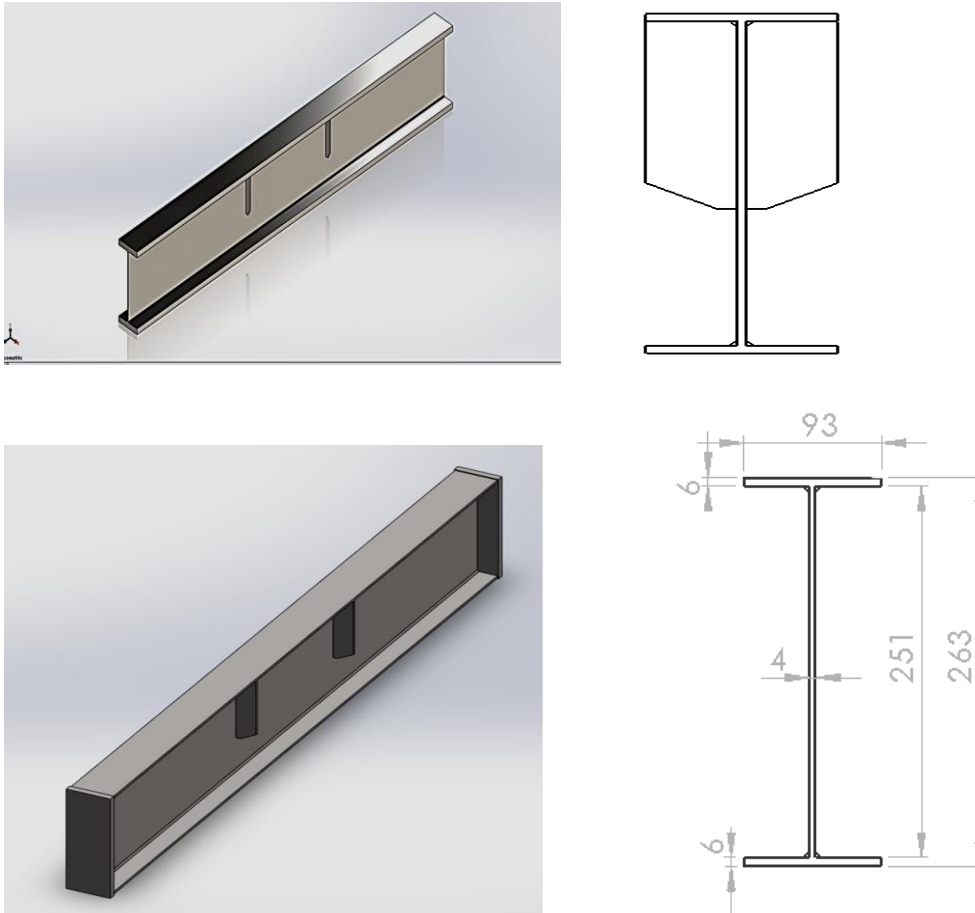


Figure 1 Side views of the I-beam (Laamanen, 2013).

SFS EN 1993-1-1 states the basic design rules for steel structure which have material thicknesses of $t \geq 3$ mm (SFS EN 1993-1-1). This part also provides supplementary provisions for the structural design of steel buildings. The part 1-1 covers general rules, basis of design, materials, durability and structural analysis, serviceability limit states and ultimate limit states (SFS EN 1993-1-1, p.10). At the ultimate limit states the designed moment resistance partial factors are outlined as follows:

$$\gamma_{M0} = 1,00$$

$$\gamma_{M1} = 1,00$$

$$\gamma_{M2} = 1,25$$

(SFS EN 1993-1-1, p. 45).

2.3.2 Throat Thickness

SFS EN 1993-1-8 outlines design methods for the design of joints that are under predominantly static loading using steel grades S235, S275, S355 and S460. It covers the basic components of a joint, connections, connected member, joint, joint configuration, rotational capacity, rotational stiffness, and structural properties of a joint and so on. According to SFS EN 1993-1-8 section 4.5.2, effective throat thickness is the height of the largest triangle that is inscribed within the fusion faces and the weld surface, measured perpendicular to the outer side of the triangle. This can simply be explained as the height of the weld measured perpendicularly from the root of the weld to the outer surface. Figure 2 describes the throat thickness of the fillet welds. SFS EN 1993-1-8 assumes that a perfect isosceles triangle is inscribed within the fillet weld. The throat thickness is indispensable when determining the throat area or the area of the fillet welds. The standard outlines that the throat thickness must not be less than 3 mm. The throat is very useful in assessing the shear resistance of the fillet welds.

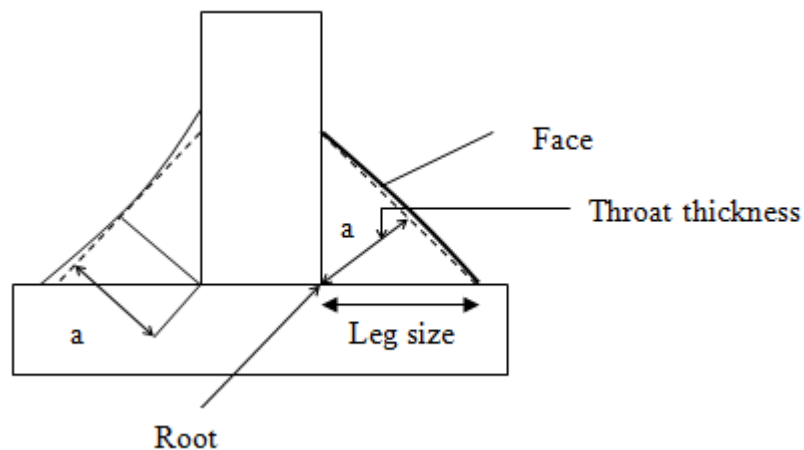


Figure 2 Throat thickness of a fillet weld based on EN 1993-1-8.

The throat thickness in Figure 2 is denoted by letter a in accordance with SFS EN 1993-1-8. Based on the details of Figure 2 the throat thickness is related to the shear strength as follows:

$$\tau_{wed} = \frac{QS}{It} = \frac{QS}{2Ia} \quad (1)$$

In this case the thickness of the section t is replaced by the total throat thickness as (2a).

Q = equals the designed shear force.

(SFS EN 1993-1-5, 51).

Also,

$$\tau_{wed} = \frac{f_u / \sqrt{3}}{\beta_w \gamma_{M2}} \quad (2)$$

(SFS EN 1993-1-8, p. 44).

Where f_u = ultimate tensile strength which is estimated to be 1100 N/mm^2 .

Equating (1) and (2) yield

$$a = \frac{\sqrt{3} \beta_w QS \gamma_{M2}}{2 I f_u} \quad (3)$$

The correlation factor β_w of the fillet weld is taken as 1 and it is based on the strength of the base material (Björk, 2013).

Given that $Q = 300 \text{ kN}$, $f_u = 980 \text{ N/mm}^2$, $\gamma_{M2} = 1,25$, $\beta_w = 1$, $\bar{y} = 128,5 \text{ mm}$, $A_{ft} = 558 \text{ mm}^2$

$$S = \bar{y} A_{ft} = 71703 \text{ mm}^3$$

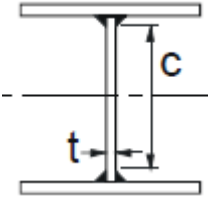
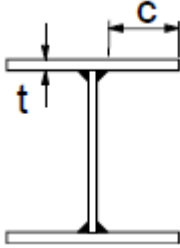
$$a = \frac{(\sqrt{3})(300 \times 10^3)(71703)(1,25)}{2(23,7 \times 10^6)(980)} = 1,0 \text{ mm}$$

The throat thickness is too small so the minimum requirement shall be used in subsequent calculations.

2.3.3 Local Buckling Check

Due to high strength to weight ratio the I-beam is made of thin plates. Considering the slenderness of the I-beam which is under compression, local buckling may occur if the width to thickness ratio is too high (Wang, 2002). Under uniform compression the stress distribution is uniform. Once local buckling sets in the stress distribution is no longer uniform and the load is resisted by areas of high stiffness (Wang, 2002). Load-carrying capacity of steel members subjected to bending (in the absence of axial load) depends mostly on the local stability of the compressed flanges and the bending webs of the cross section (Juhás, 2009). Local buckling is checked to see if the width to thickness ratio exceeds required limit. If the limit is not exceeded it means local buckling is not a problem to be considered. Local buckling is checked with Eurocode 3 recommendations as follows:

Table 3 Eurocode 3 recommendation for checking width-to-thickness ratios.

Internal compression part		Outstand flanges	
			
Class	Part subject to bending	Part subject to compression	
3 (internal)	$c/t \leq 124\varepsilon$		
1 (outstand flanges)		$c/t \leq 14\varepsilon$	
$\varepsilon = \sqrt{235/f_y} = 0,495$			

Verification:

(Web)

$$c/t \leq 124\varepsilon$$

throat thickness, $a = 3$ mm (minimum requirement)

From Figure 4, $c = 251 - 2\sqrt{2}a = 242,5$ mm. Thickness of web $t = 4$.

$$242,5/4 \leq 124 \cdot 0,495 \Rightarrow 60,63 < 61,38.$$

The condition $c/t \leq 124\varepsilon$ is satisfied. Local buckling does not occur in the web.

(Outstand flange)

$$c/t \leq 14\varepsilon,$$

$$c = (93 - 4)/2 - \sqrt{2} a = 40,25,$$

Flange thickness $t = 6$, $c/t = 6,71 < 14\varepsilon = 6,93$

The beam has a class 3 web and class 3 flanges.

Flange-induced buckling in the plane of the web

SFS EN-1993-1-5 gives the following criterion for preventing the compression flange buckling in the plane of web:

$$\frac{h_w}{t_w} \leq k \frac{E}{f_{yf}} \sqrt{\frac{A_w}{A_{fc}}} \quad (4)$$

where

A_w is the cross section area of the web;

A_{fc} is the effective cross section area of the compression flange;

f_{yf} is the yield strength of flange;

h_w is the depth of the web;

t_w is the thickness of the web

k equals to 0,3, 0,4 and 0,55 for plastic rotation, plastic moment resistance and elastic moment resistance respectively.

(SFS EN-1993-1-5, p. 29).

Verification:

From Figure 1, $h_w = 251$ mm, $t_w = 4$ mm, $b_f = 93$ mm, $t_f = 6$ mm.

$$\frac{251}{4} \leq 0,55 \cdot \frac{210000}{960} \sqrt{\frac{1004}{558}}$$

$$62,75 \leq 161,38$$

It implies that the height to thickness ratio of web (h_w / t_w) satisfies the above condition in equation (4).

2.3.4 Effective Cross Section Properties

SFS EN 1993-1-5 outlines the procedure for determining the effective cross section properties. The standard recommends the use of A_{eff} , I_{eff} and W_{eff} for assessing the effects of plate buckling. For plates without longitudinal stiffeners the effective plate area of the compression zone of a plate with gross cross sectional area is given A_c is given as

$$A_{c,eff} = \rho A_c \tag{5}$$

where ρ is the reduction factor.

(SFS EN 1993-1-5, p.17)

Figure 3 shows the effective plate cross sections of the I-beam.

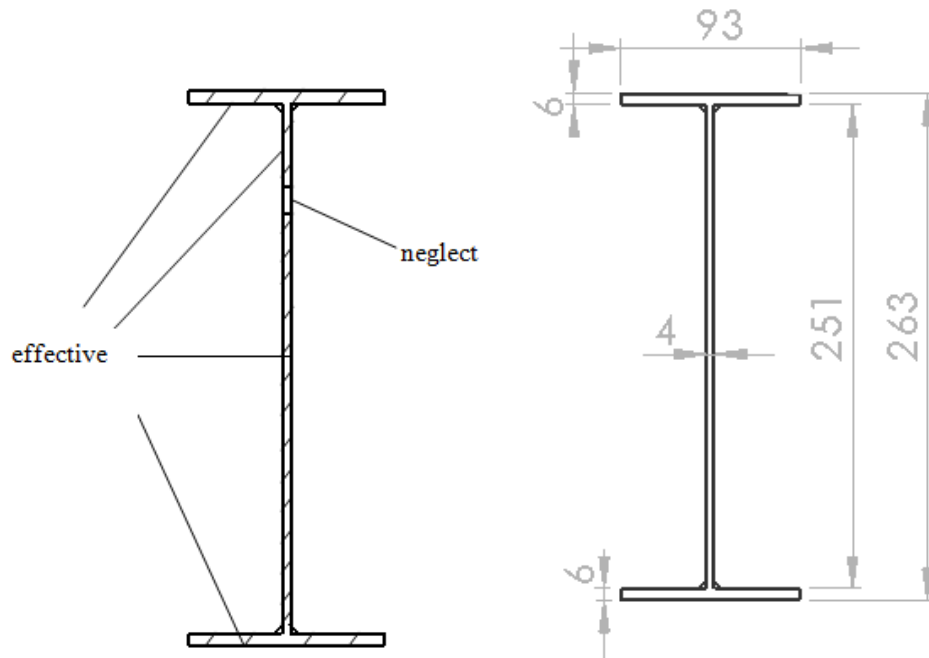


Figure 3 Effective plate areas

From Figure 3, $b = 93 \text{ mm}$, $t_f = 6 \text{ mm}$, $t_w = 4 \text{ mm}$, $h_w = 251 \text{ mm}$, $h = 263 \text{ mm}$

Nominal Area, $A = 2bt_f + h_w t_w$

$$A = 2120 \text{ mm}^2$$

Based on Figure 3 and Appendix 1 the effective plate width b_{eff} can be determined. The reduction factor ρ is determined in order to define the effective parts of the I-beam.

The procedure is as follows:

Web effectiveness:

$$b_{eff} = \rho \bar{b} / 1 - \psi \quad (6)$$

For plate elements without longitudinal stiffeners ρ is given as follow:

$$\rho = 1,0 \text{ for } \bar{\lambda}_p \leq 0,673 \quad (6.1)$$

$$\rho = \frac{\bar{\lambda}_p - 0,055(3 + \psi)}{\bar{\lambda}_p^2} \leq 1,0 \text{ for } \bar{\lambda}_p > 0,673, \text{ where } (3 + \psi) \geq 0 \quad (6.2)$$

$$\text{where } \bar{\lambda}_p = \frac{\bar{b} / t}{28,4 \varepsilon \sqrt{k_\sigma}} \quad (7)$$

$\bar{b} = b_w$ and $k_\sigma =$ buckling factor corresponding to ψ (Appendix 1)

(SFS EN1993-1-5, p. 15)

$$a = 3 \text{ mm}, t_w = 4 \text{ mm}, h_w = 251 \text{ mm}, \bar{b}_w = h_w - 2\sqrt{2}a = 242,5 \text{ mm}.$$

Stress distribution of the web implies that $\psi = -1, k_\sigma = 23,9$.

$$\Rightarrow \bar{\lambda}_p = \frac{242,5 / 4}{28,4 \cdot 0,495 \sqrt{23,9}} = 0,88$$

$\bar{\lambda}_p = 0,88 > 0,673$, so $\rho = 0,99$, according to (3.2).

$$b_{eff} = \rho h_w / 2 = 0,99 \cdot 251 / 2 = 124,2 \text{ mm}$$

$$b_{e1} = 0,4 b_{eff} = 49,68 \text{ mm}$$

$$b_{e2} = 0,6 b_{eff} = 74,5 \text{ mm}$$

$$b_n = \frac{h_w}{2} - b_{e1} - b_{e2} = \frac{251}{2} - 49,2 - 73,8 = 1,3 \text{ mm}$$

$b_n =$ height of non-effective part of the web

Outstand flange effectiveness:

$$b_{eff} = \rho c \quad (8)$$

$$\rho = 1,0 \text{ for } \bar{\lambda}_p \leq 0,748 \quad (8.1)$$

$$\rho = \frac{\bar{\lambda}_p - 0,188}{\bar{\lambda}_p} \leq 1,0 \quad \text{for } \bar{\lambda}_p > 0,748 \quad (8.2)$$

$$\bar{b} = (93 - 4) / 2 - \sqrt{2} a = 40,25 \text{ mm}, t_f = 6 \text{ mm}, \psi = 1, k_\sigma = 0,43 \text{ for } 1 \geq \psi \geq -3$$

because $1 > \psi \geq 0$ is not valid for the flange stress ratio $\psi = 1$.

$$\bar{\lambda}_p = \frac{40,25 / 6}{28,4 \cdot 0,495 \sqrt{0,43}} = 0,727$$

$\bar{\lambda}_p = 0,727 < 0,748 \Rightarrow \rho = 1,0$. Compression flange is completely effective. The effective area of the I-beam is given by the expression below.

$$A_{eff} = 2bt_f + h_w t_w - (t_w b_n) = 2120 - (4 \cdot 1,3) = 2115 \text{ mm}^2.$$

Moment of inertia

$$t_f = 6, b = 93, h = 263, h_{eff} = 261,7, t_w = 4, h_w = 251, h_{w,eff} = 249,7$$

$$I = \frac{1}{12} (b_f h^3) - \frac{1}{12} (b_f - t_w) h_w^3$$

$$I = 23,7 \times 10^6 \text{ mm}^4.$$

$$I_{eff} = 23,43 \times 10^6 \text{ mm}^4$$

$$I_z = \frac{2t_f b^3}{12} + \frac{(h - 2t_f) t_w^3}{12}$$

$$I_z = 805696 \text{ mm}^4$$

Elastic Section Modulus

Section 4.3 (4) of SFS EN 1993-1-5 requires the calculation of effective section modulus W_{eff} for the beam cross section assuming the cross section is subject to only bending stresses. This clause also allows the computation of effective section moduli for biaxial bending. The elastic section modulus about the neutral axis is given by moment of inertia about the neutral axis (major axis) divided by the centroid of the cross-section (Egor, 1998, p. 339). For class 3 cross-section the elastic section modulus is denoted as W_{el} . In subsequent calculations the effective section modulus about the effective neutral axis will be denoted as $W_{el,t}$

$$W_{el,t} = I_{eff} / e^t$$

$$W_{el,c} = I_{eff} / e^c$$

where e^t = centroid of effective cross section = $(h - 1,3) / 2$

and $e^c = h - e^t$

$$W_{el,t} = 23,43 \times 10^6 / 130,85 = 179060 \text{ mm}^3$$

$$\text{and } W_{el,c} = 23,43 \times 10^6 / 132,15 = 177299 \text{ mm}^3.$$

Plastic Section Modulus

In accordance with Gorenc, Tinyou and Syam's (2005) formula, the plastic section modulus of an I-beam is given as

$$Z = 2(A_b y_b) = Ay_b \quad (9)$$

(Gorenc, Tinyou and Syam, 2005, p.267).

Where A is the area of the I-beam and y_b is the distance between the plastic neutral axis the centroid of the half section (A_b) in Figure 4.

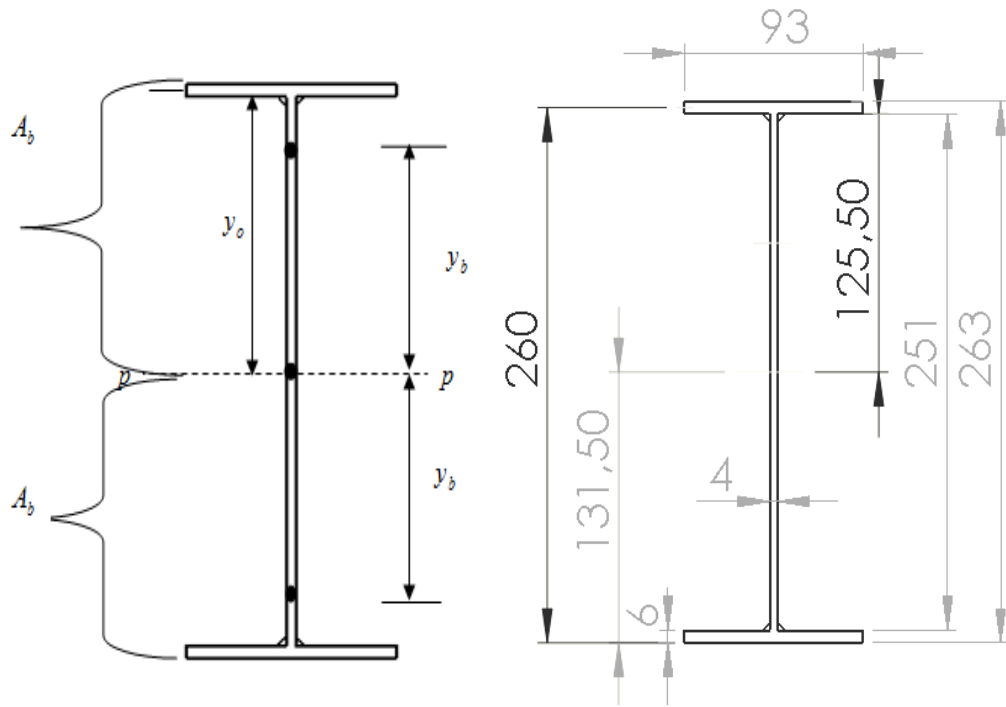


Figure 4 Computation of plastic section modulus for doubly symmetric I-beam.

The left figure in Figure 4 is a modified version of Gorenc, Tinyou and Syam's (2005) figure for computing plastic section modulus. Before calculating the plastic section modulus, the centroid positions of each half section is calculated.

Centroid of top half area about the plastic neutral axis $p-p$:

$$\bar{A} y = \sum A y_i \quad (10)$$

$$y_0 = \frac{1}{2} \times 251 = 125.5$$

$$A_1 = 93 \times 6 = 558, \quad y_1 = 260$$

$$A_2 = 125,5 \times 4 = 502, \quad y_2 = (131,5 + \frac{1}{2} \times 125,5) = 194,25$$

$$\begin{aligned} \bar{y} &= \frac{(93 \times 6) \times 260 + (125,5 \times 4) \times 194,25}{(93 \times 6) + (125,5 \times 4)} \\ &= 228,86 \text{ mm} \end{aligned}$$

Centroid of the bottom half area about the plastic neutral axis $p-p$:

$$A_1 = 93 \times 6 = 558, \quad y_1 = 3$$

$$A_2 = 125,5 \times 4 = 502, \quad y_2 = (\frac{1}{2} \times 125,5 + 6) = 68,75$$

$$y = \frac{(93 \times 6) \times 3 + (125,5 \times 4) \times 68,75}{(93 \times 6) + (125,5 \times 4)}$$

$$= 34,14 \text{ mm}$$

The distance between the centroids of the two-half areas can now be estimated as follows:

$$2 y_b = 228,86 - 34,14 = 194,72 \text{ mm}$$

$$\Rightarrow y_b = 97,36 \text{ mm}$$

$$\Rightarrow Z = 2120 \text{ mm}^2 \cdot 97,36 \text{ mm} = 206403 \text{ mm}^3$$

Warping and Torsional Constants

The warping and torsional constants are tabulated in Table 4 based on the parameter of the I-beam in Figure 5.

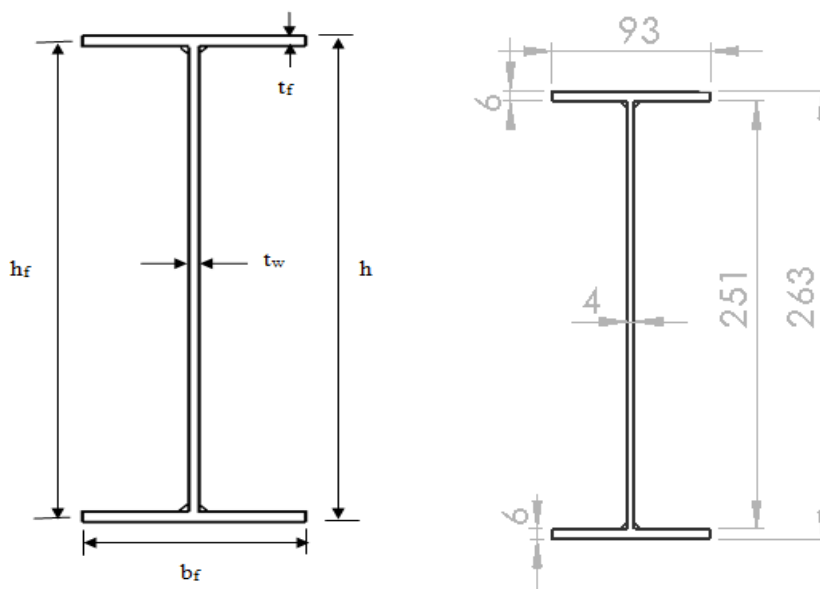


Figure 5 I- beam parameters and numerical dimensions.

The warping constant is given by the following expressions:

$$I_w = \frac{t_f h_f^2 b^3}{24} \quad (11)$$

(Hoogenboom, 2006).

which gives exactly the same answer as $I_w = 0,25h_f^2 I_z$ (12)

If $I_z = 2 \frac{b^3 t_f}{12}$ = moment of inertia of a flange.

where I_w = warping constant

Similarly, the torsional constant is given by

$$I_v = \frac{1}{3} [2bt_f^3 + (d - 2t_f)t_w^3] \quad (13)$$

where h is replaced by d .

(Lehtinen, 2005,p. 54; Gorenc, Tinyou & Syam, 2005, p. 243).

Table 4 warping and torsional constants.

t_f (mm)	t_w (mm)	h_f (mm)	b (mm)	d (mm)	I_v (mm^4)	I_w (mm^6)
6	4	(251 +3+3) = 257	93	263	18747	1328×10^7

3 FAILURE CRITERIA

3.1 General Failure Criteria

Failure of I-beam may arise as result of several factors including ductile fracture at nominal stresses within the ultimate strength of the weld (Gorenc, Tinyou & Syam, 2005). Table 5 is a list of some failure criteria at service and ultimate limits. Geometric imperfections such as voids, distortions and cracks can reduced the ultimate capacity of the I-beam. Buckling may induce structural change in the I-beam cross sections.

Table 5 Failure criteria at service limit and ultimate limit.

Service Limit Failure	Ultimate Limit Failure	
	No Cracks	Cracks
Deflection	Buckling	Fatigue
Vibration	Plasticity	Brittle Fracture
Local yielding	Cyclic Plastic	Stress Corrosion
	Creeping	

3.2 Deflection

When a beam is loaded, it may deflect vertically or horizontally depending on the position of the applied load. The I-beam is loaded as shown in Figure 6. The two equal concentrated loads are symmetrically placed and the maximum deflection is computed with equation 14.

$$\delta_{\max} = \frac{Pl}{24EI} (3L^2 - 4l^2) \quad (14)$$

where δ_{\max} is the deflection at center

l = the distance between the loading points and the reaction supports.

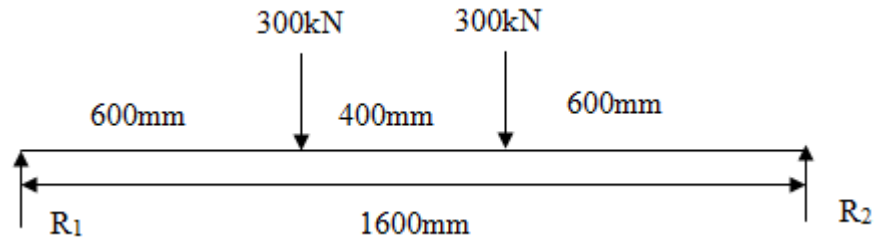


Figure 6 Loading of the I-beam.

Given that $l = 600$ mm, $P = 300$ kN, $L = 1600$ mm, $I = 23,7 \times 10^6 \text{ mm}^4$,

$$E = 210000 \text{ N/mm}^2$$

$$\Rightarrow \delta_{\max} = 9,4 \text{ mm}$$

3.3 Elastic Limit

Elastic limit is maximum stress that the beam can withstand without any measurable permanent deformation. Within the elastic limit the beam can regain its shape or stability when the applied load is removed. Figure 7 shows the distribution of stresses when the elastic limit is reached. The beam may yield when the applied stress reaches or exceeds the yield limit of the beam. In full elasticity, the outer fibres of the cross-section are stressed to the yield point but the interior cross-section remains elastic (David, 2006). In this case, the applied moment becomes equal to the yield moment (Williams, 2001).

The elastic moment capacity of the I-beam is calculated with the following formula:

$$\text{Elastic limit, } \sigma_y = \frac{M_y}{W_{el}} \quad (15)$$

where

σ_y = yield strength

M_y = elastic moment capacity

$W_{el} = W_{el,t}$ = elastic section modulus

The elastic moment capacity can be computed as follows:

$$M_y = 960 \text{ N/mm}^2 \times 179060 \text{ mm}^3 = 172 \text{ kNm.}$$

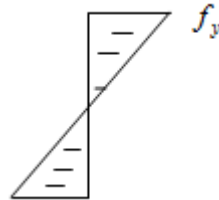


Figure 7 Stress distribution diagram at the elastic limit.

3.4 Stability

The stability of the beam is affected by local buckling as local mode and flexural buckling as global mode. Local buckling has been treated in chapter 2. In the subsequent sections flexural buckling and flexural capacities of the beam are covered.

Flexural buckling as global mode

Lateral buckling of a steel beam occurs when the beam is loaded about its major axis and deforms laterally (twisting) due to low torsional stiffness and low bending stiffness about the minor axis (Wang, 2002). In other words, when the beam is laterally unrestrained, bending of the beam about its major axis is accompanied by lateral displacement about its weak axis and twist (Wang, 2002). Sufficient lateral and torsional restraints must be provided to prevent lateral torsional buckling (Wang, 2002). When the beam fails as a result of lateral torsional buckling, the maximum bending moment in the beam is lower than the plastic moment capacity of the cross section (Wang, 2002).

Investigation of buckling behaviour requires proper definitions of boundary conditions and it is up to the engineer to decide whether the panels are stiffened or unstiffened (Dubina & Ivanyi, 1999). According to Dubina and Ivanyi (1999) the designer has to decide whether flanges will offer enough stiffness to prevent lateral displacements and rotations at the longitudinal edges of the plate.

Factors affecting lateral stability according to Institute for steel Development and Growth (INSDAG):

- Support conditions

The support conditions have influence on the lateral-torsional buckling capacity. The lateral restraints provided by simply supported condition is not adequate compared to a fixed support. Warping restraints, twisting restraints and lateral deflection restraints increase the load carry capacity.

- Effective length

For a simply supported beam, the effective length is the span of the two

supports. In this case the effective length factor is 1 but for braced members, the effective length factor may be lower. The length is higher when there is less restraint.

- Material properties

Material properties such as modulus of elasticity or toughness may increase the load carrying capacity though high slenderness of the beam is still a problem.

- Level of application of transverse load

Concentrated loads above the shear center may tend to have destabilising effect. This causes additional overturning moment. If the concentrated load is below the shear center it may have a stabilizing effect.

- Effect of cross sectional shape

The type of cross-section influences the stability. Box sections have higher stability than I-beams due to higher torsional stiffness.

- Type of loading

The type of loading determines the moment distribution. The beam with variation in moment gradient may tend to have higher loading capacity than the one with the same maximum moment which is uniform along its length.

- Imperfections

Initial imperfections present in the beam may reduce the load carrying capacity. Lack of straightness may be worsened when the load is applied.

- Residual stresses

The present of residual stresses tend to increase distortion of I-beam and may increase the occurrence of failure. Yielding of the section starts at lower moments and spreads quickly when the moment is increased.

3.5 Capacities of I-Beam

3.5.1 Buckling Capacity

The effects of flexural stresses include buckling, twisting and lateral displacement of the beam members. These phenomena are illustrated by Figures 8 and 9. In Figure 8 the top flange buckles outward as moments are applied at each end of the I-section. Figure 9 shows twisting of the web and lateral displacement.

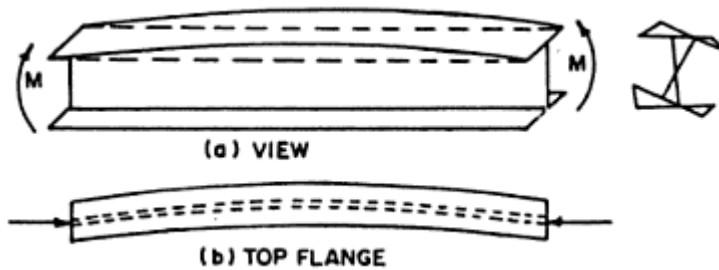


Figure 8 Lateral buckling of unrestrained I-beam (Punmia, Ashok & Arun, 1998, p.243)

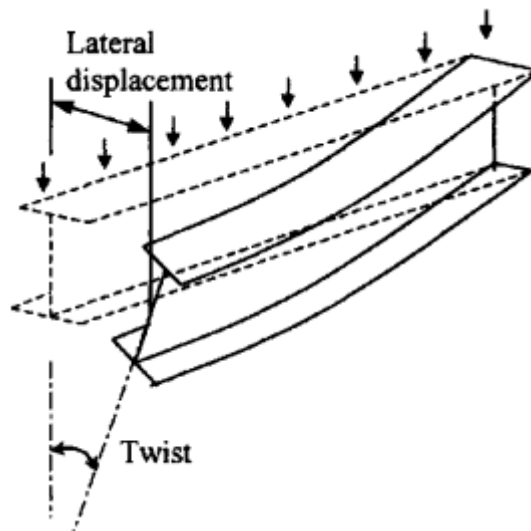


Figure 9 Lateral torsional buckling of an unrestrained beam (Wang, 2002, p.13)

In order to determine the lateral buckling capacity $M_{b,Rd}$ the buckling curve is determined and the non-dimensional slenderness χ_{LT} (for lateral buckling) is chosen. The value of the non-dimensional slenderness corresponds to the reduction factor for the moment resistance. For the welded I-section the condition $h/b < 2$ or $h/b > 2$ must be satisfied which may correspond to buckling curve c or d of the standard (SFS EN 1993-1-1, p.58, 61). Appendix 2 contains the buckling curves. The critical buckling moment M_{cr} is also essential for determination of the reduction factor. The elastic critical moment for lateral-torsional buckling is used to determine the buckling strength of I-beam members (Ioannis & Theodore, 2010). The elastic critical moment and buckling reduction factors are calculated as follows:

$$\text{but } M_{cr} = C_1 \frac{\pi^2 EI_z}{kL^2} \left[\sqrt{\left(\frac{k}{k_\omega}\right)^2 \frac{I_w}{I_z} + \frac{(kL)^2 GI_v}{\pi^2 EI_z} + (C_2 Z_g - C_3 Z_j)^2} + (C_2 Z_g - C_3 Z_j) \right] \quad (16)$$

C_1, C_2 and C_3 are constants, which correspond to the moment diagram or loading case

I_v = torsional constant

I_w = warping constant

I_z = Second moment of inertia (of I-beam) about the minor axis or weak axis

L = length of the I-beam (between points with lateral restraints).

k and k_ω are effective length factors

Z_g = the distance between the point of load application and the shear center,

which coincides with centroid for the doubly symmetric I-beam.

$Z_j = 0$, since Z_g coincides with the centroid

(Lehtinen, 2005, p.51 & SN003a-EN.pdf).

Figure 10 makes the aforementioned conditions hold and the equation takes a simplified form.

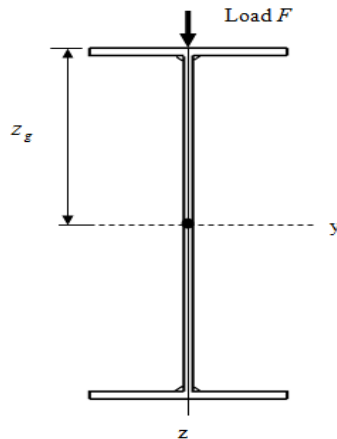


Figure 10 Point of application of transverse load.

The formula then reduces to

$$M_{cr} = C_1 \frac{\pi^2 EI_z}{kL^2} \left[\sqrt{\left(\frac{k}{k_\omega} \right)^2 \frac{I_w}{I_z} + \frac{(kL)^2 GI_v}{\pi^2 EI_z} + (C_2 Z_g)^2} + (C_2 Z_g) \right] \quad (17)$$

From equation (17) the critical buckling moment can be calculated as follows:

Table 6 Loading constants and effective length factors (Lehtinen, 2005, p.53).

k	k_ω	C_1	C_2	C_3
1	1,0	1,046	0,430	1,120
1	0,5	1,046	0,430	1,120

The loading constants were chosen based on the shape of the moment distribution. The effective length factors are based on the nature of the support conditions. Elastic critical moment is estimated for when warping is free and also when warping is restricted, to account for the end plates of the I-beam. For the loading case in Figure 6, the shear and bending moment diagrams are depicted in Figure 11. The designed bending moment M_{Ed} is 180 kNm.

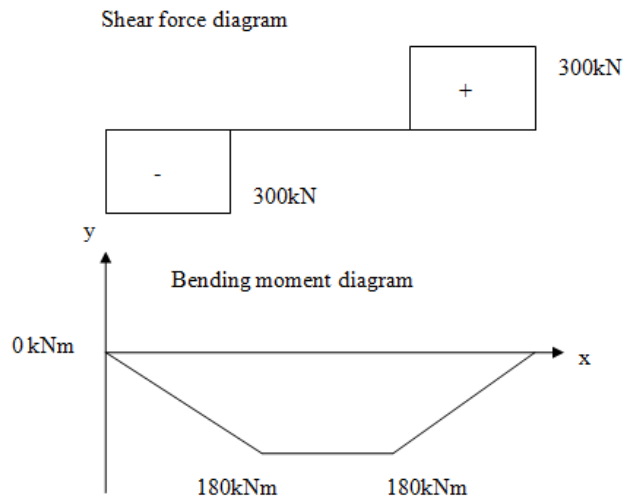


Figure 11 Shear and Moment distribution.

Given $L = 1600$ mm, $Z_g = 131,5$ mm, $I_v = 18747$ mm⁴, $I_\omega = 1328 \times 10^7$ mm⁶,

$$M_{cr,1} = 1,046 \cdot \frac{\pi^2 * 210000 * 805696}{1600^2} \times$$

$$\left[\sqrt{\frac{1328 \times 10^7}{805696} + \frac{(1600)^2 * 81000 * 18747}{\pi^2 * 210000 * 805696}} + (0,430 * 131,5)^2 + (0,430 * 131,5) \right]$$

$$= 139,8 \text{ kNm.}$$

$$\bar{\lambda}_{LT} = \sqrt{\frac{W_y f_y}{M_{cr}}} \quad (18)$$

$\bar{\lambda}_{LT}$ = non-dimensional slenderness.

(SFS EN 1993-1-1, p. 61).

Given that $f_y = 960 \text{ N/mm}^2$, $W_y = W_{el,t} = 179060 \text{ mm}^3$ and $M_{cr} = 139,8 \times 10^6 \text{ Nmm}$

$$\bar{\lambda}_{LT} = \sqrt{\frac{179060 \times 960}{139,8 \times 10^6}} = 1,11$$

Lateral-torsional buckling curve

For the beam, $h/b > 2$, therefore the appropriate buckling curve corresponds to curve d which is given by the standard (Appendix 2). To reduce error of reading from the curve, the buckling reduction factor χ_{LT} is calculated as follows:

$$\chi_{LT} = \frac{1}{\phi_{LT} + \sqrt{\phi_{LT}^2 - \beta \bar{\lambda}_{LT}^{-2}}}, \begin{cases} \chi_{LT} \leq 1,0 \\ \chi_{LT} \leq \frac{1}{\bar{\lambda}_{LT}^2} \end{cases} \quad (19)$$

$$\text{where } \phi_{LT} = 0,5 \left[1 + \alpha_{LT} (\bar{\lambda}_{LT} - \bar{\lambda}_{LT,0}) + \beta \bar{\lambda}_{LT}^{-2} \right] \quad (20)$$

and $\bar{\lambda}_{LT,0} = 0,4$ (maximum value)

(SFS EN 1993-1-1, p. 62).

Given that $\beta = \beta_w = 1$, $\alpha_{LT} = 1$ and $\bar{\lambda}_{LT} = 1,11$, the lateral buckling reduction factor, χ_{LT} can be determined as follows:

$$\Rightarrow \phi_{LT} = 0,5 \left[1 + (1,11 - 0,4) + (1,11^2) \right]$$

$$= 1,47$$

$$\Rightarrow \chi_{LT} = \frac{1}{1,47 + \sqrt{1,47^2 - 1,11^2}}$$

$$= 0,41$$

Also, when k_ω is taken as 0,5 (Table 6), buckling reduction factor, χ_{LT} is calculated as follows:

$$M_{cr,2} = 1,046 \frac{\pi^2 \times 210000 \times 805696}{1600^2} \times$$

$$\left[\sqrt{\left(\frac{1}{0,5}\right)^2 \frac{1328 \times 10^7}{805696} + \frac{1600^2 \times 81000 \times 18747}{\pi^2 \times 210000 \times 805696} + (0,430 \times 131,3)^2 + (0,430 \times 131,5)^2} \right]$$

$$= 221kNm.$$

$$\Rightarrow \bar{\lambda}_{LT} = 0,88 \text{ and } \phi_{LT} = 1,13.$$

$$\Rightarrow \chi_{LT} = \frac{1}{1,13 + \sqrt{1,13^2 - 0,88^2}}$$

$$= 0,54$$

This means that the buckling reduction for the loading case is within 0,41 and 0,54. The value of χ_{LT} means that buckling is inevitable and it needs to be reduced to prevent any probable failure.

The designed buckling resistance moment $M_{b,Rd}$ of a laterally unrestrained beam member is given as

$$M_{b,Rd} = \frac{\chi_{LT} W_y f_y}{\gamma_{M1}} \quad (21)$$

For uniform member in bending,

$$\frac{M_{Ed}}{M_{b,Rd}} \leq 1,0 \quad (22)$$

(SFS EN 1993-1-1, p. 60).

Given that $W_y = W_{el,t} = 179060 \text{ mm}^3$, $f_y = 960 \text{ N/mm}^2$,

when $\chi_{LT} = 0,41 \Rightarrow M_{b,Rd} = 70,5 \text{ kNm}$

when $\chi_{LT} = 0,54 \Rightarrow M_{b,Rd} = 93 \text{ kNm}$

The maximum lateral buckling capacity is 93 kNm.

3.5.2 Plasticity

Fully plastic moment capacity of the I-beam is the maximum value of the bending moment that the beam can resist in fully yielded condition (Gorenc, Tinyou & Syam, 2005). At this point all the cross-section is fully stressed to the yield stress without offering the slightest increase in resistance (Gorenc, Tinyou & Syam, 2005). When the plastic moment is reached there is a moment distribution as shown in Figure 12. Lateral-torsional buckling can be eliminated by additional supports. If the beam is prevented from both local and lateral-torsional buckling, failure may occur when the maximum bending moment in the beam has reached the plastic moment capacity (Wang, 2002). At this stage if the load is gradually increased a plastic hinge will be formed at the extreme compression or tension fibres of the weakest section (plastic theory of bending, CODECOGS). This will eventually lead to a complete collapse. In reality a plastic hinge will allow rotation to happen (Gorenc, Tinyou & Syam, 2005). The maximum bending moment of a fully restrained beam in the absence of axial force is given as:

$$M_{p \max} = \phi f_y Z \quad (23)$$

where

Z = plastic section modulus

$M_{p \max}$ = maximum plastic moment

ϕ = shape factor

(Gorenc, Tinyou & Syam, 2005, p. 267).

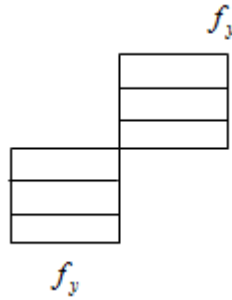


Figure 12 Plastic moment distribution (Gorenc, Tinyou & Syam, 2005, p. 268).

$$\phi = \frac{M_p}{M_y} = \frac{Z}{W_{el}} \quad (28)$$

where

M_p = plastic moment

W_{el} = elastic section modulus

(Williams, 2001, p.98).

$$\phi = \frac{206403}{179060} = 1,15$$

Table 7 summarises the plastic moment capacities and the shape factor.

Table 7 Plastic capacity and shape factor for I-beam.

f_y	Z	$M_p = f_y Z$	ϕ	$M_{p\max} = \phi f_y Z$
960 N/mm ²	206403 mm ³	198 kNm	1,15	228 kNm

The plastic section modulus $Z = 1,15 W_{el}$. The maximum designed plastic capacity $M_{p\max}$ in a fully restrained condition is 228 kNm. If the I-beam were laterally supported, then, beyond 228 kNm the beam may not offer any resistance to plastic deformation. Full plastic moment in an unrestrained condition M_p is 198 kNm. Considering the

slenderness of the I-beam, plastic moment capacity can occur shortly after exceeding the elastic moment capacity. Within the plastic capacity rotation is limited.

3.6 Fatigue Strength

SFS EN 1993-1-9 is concerned with the methods for assessing the fatigue resistance of members, connections and joints that are subject to fatigue loading. “The fatigue strengths apply to structures operating under normal atmospheric conditions and with sufficient corrosion protection and regular maintenance. The effect of sea water corrosion is not covered. Microstructural damage from high temperature ($> 150\text{ }^{\circ}\text{C}$) is not covered.” SFS EN 1993-1-9, p. 6).

Fatigue is the phenomenon of crack initiation and growth through a structural part due to the effects of fluctuating stresses (SFS EN 1993-1-9). Fatigue strength can then be explained as the materials resistance against such phenomena which can lead the structure into failure. Stress concentrations at the hot spot areas such as the fillet weld toes and the shear centre may cause the structure to fail. The weld profile also has an influence on the fatigue strength of the structure (Maddox, 2002). The fatigue strength is also dependent on number of stress cycles to failure, that the structure can endure (Radaj, 1990).

The fatigue strength calculations are based on the nominal stress values. The standard defines nominal stress as the stress in parent material or stress in the weld which is located near a crack location in accordance with the elastic principle (SFS EN 1993-1-9). The fatigue strengths are traced from fatigue strength curves (S-N curves) in Appendices 3 and 4. For direct stress ranges, SFS EN 1993-1-9 recommends stress category (line) 36 for determination of fatigue strength in the fillet welds. Since the top flange and top fillet welds carry transverse load, the stress detail category corresponding to the bending members is 80 (Appendices 3 and 4). The following rules are recommended by SFS EN 1993-1-9 for determination of fatigue strength:

For constant amplitude nominal stresses fatigue strength can be determined as follows:

$$\Delta\sigma_R^m N_R = \Delta\sigma_c^m 2 \times 10^6 \quad (24)$$

with $m = 3$ for $N \leq 5 \times 10^6$ (Appendix 3)

$\Delta\sigma_c$ is reference value of stress at 2million cycles.

with $m = 5$ for $N \leq 5 \times 10^8$ (Appendix 4)

$$\Delta\sigma_D = 0,737\Delta\sigma_c \quad (25)$$

where $\Delta\sigma_D =$ constant amplitude fatigue limit.

The fatigue resistance of the I-beam decreases until the constant amplitude fatigue limit. Below the constant amplitude fatigue limit no cracks occur (SFS EN 1993-1-9). For stresses above or below the constant amplitude fatigue limit $\Delta\sigma_D$ the fatigue strength must be based on the extended fatigue strength curves as follows:

$$\Delta\sigma_R^m N_R = \Delta\sigma_c^m 2 \times 10^6 \text{ with } m = 3 \text{ for } N \leq 5 \times 10^6$$

$$\Delta\sigma_R^m N_R = \Delta\sigma_D^m 5 \times 10^6 \quad (26)$$

with $m = 5$ for $5 \times 10^6 \leq N \leq 10^8$

$$\Delta\sigma_L = 0,549\Delta\sigma_D \quad (27)$$

where $\Delta\sigma_L =$ cut of limit.

Maximum stresses

The stresses are determined based on nominal values. With the absence of axial load, the designed bending stress (nominal) is given by

$$\sigma_{\max} = \frac{Mc}{I}$$

where σ_{\max} = maximum stress, I = moment of inertia about the neutral axis, c = centroid

For high cycle fatigue ($R= 6,6$), $\Delta F = F_{w,Rd} / 4$

where $F_{w,Rd}$ = designed shear force = 300 kN.

$$\sigma_{\max} = \frac{(75 \cdot 10^3 \text{ kN} \cdot 600 \text{ mm}) \cdot 131,5 \text{ mm}}{23,7 \cdot 10^6 \text{ mm}^4} = 250 \text{ MPa}$$

Let $\Delta\sigma_R = \sigma_{\max} = 250 \text{ N/mm}^2$

Then, from equation (24), the nominal fatigue life for the bending stress range can be calculated as follows:

$$N_R = \frac{\Delta\sigma_c^m}{\Delta\sigma_R^m} \cdot 2 \times 10^6$$

$$N_R = \frac{(80 \text{ N/mm}^2)^3}{(250 \text{ N/mm}^2)^3} \cdot 2 \times 10^6 \text{ cycles}$$

$$\Rightarrow N_R = 65536 \text{ cycles}$$

For a member under bending the fatigue life is just 65538 cycles. Similarly, the nominal value of the designed shear stress can be used to estimate the fatigue life due to shear stresses. The nominal value of maximum (designed) shear stress τ_{Ed} of the I-beam is also given by the following formula:

$$\tau_{\max} = \tau_{Ed} = \frac{QS}{It} \quad (28)$$

$$t = 4mm,$$

$$Q = 75 kN, \text{ (one-fourth of the shear force).}$$

$$y_1 = 128,5mm, y_2 = 62,75mm$$

$$S = A_1 y_1 + A_2 y_2 = 103203,5mm^3$$

$$\tau_{\max} = 82 MPa$$

The largest nominal stress which is mainly the bending stress is used with reference value (detail category) to plot fatigue graph for the I-beam. The next table gives the fatigue information for bending stress range while Figure 13 shows the fatigue strength curve for the bending stress range.

Table 8 Data for fatigue strength curve.

Bending stress $\Delta\sigma_{\max}$ (N/mm^2)	250	65536 cycles
Detail category (reference value) $\Delta\sigma_c$ (N/mm^2)	80	2×10^6 cycles
Constant amplitude fatigue limit $\Delta\sigma_D = 0,737\Delta\sigma_c$ (N/mm^2)	58,96	5×10^6 cycles
cut- off limit $\Delta\sigma_L = 0,549\Delta\sigma_D$ (N/mm^2)	32,4	1×10^8 cycles

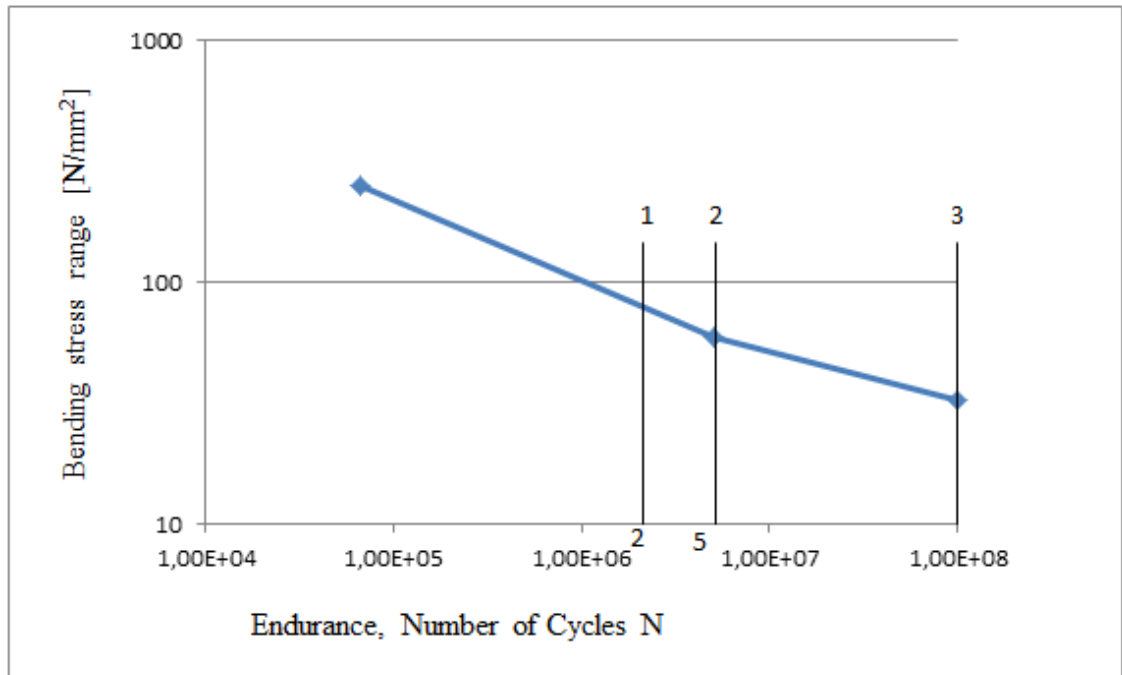


Figure 13 Fatigue strength curve for bending stress ranges.

- 1 Detail category
- 2 Constant amplitude fatigue limit
- 3 Cut-off limit

Fatigue life assessment with crack propagation equation

The crack propagation equation can be used to determine the fatigue life of a crack growth from the onset to the final crack size. The crack growth rate per cycle, da/dN is expressed as a function of the cyclic stress intensity factor at the crack tip, ΔK (Meyers & Chawla, 2009).

Under cyclic conditions, crack growth is given by the Paris-Erdogan equation:

$$da / dN = C\Delta K^m \quad (29)$$

$$\Delta K = \Delta\sigma M_k Y(a)\sqrt{\pi a} \quad (30)$$

(Hobbacher, 2013, p.33, 92).

where a is the crack length, N is the number of cycles, ΔK is the cyclic stress intensity factor, C and m are empirical material constants, $Y(a)$ is a constant that depends on the crack opening mode and geometry of the specimen, corresponds to the structural hot spot stress $\Delta\sigma_{h.spot}$ recommended by IIW. M_k is stress intensity magnification factor. For bending stress, $M_k > 1$ (Hobbacher, 2013).

According to SAE (1988) when the applied stress is lowered, critical crack size increases and failure is delayed. Fracture mechanics can be used to estimate the life spent in growing a crack from an initial size to a critical size (SAE, 1988). The crack growth behaviour is depicted schematically in Figure 14. When K_{IC} is reached the critical crack size can be computed by the equation below.

$$a_{cr} = \frac{K_{IC}^2}{\pi\sigma^2[Y(a)]^2} \quad (31)$$

where

a_{cr} = critical crack size

K_{IC} = fracture toughness in mode I loading

(Meyers & Chawla, 2009, p.405).

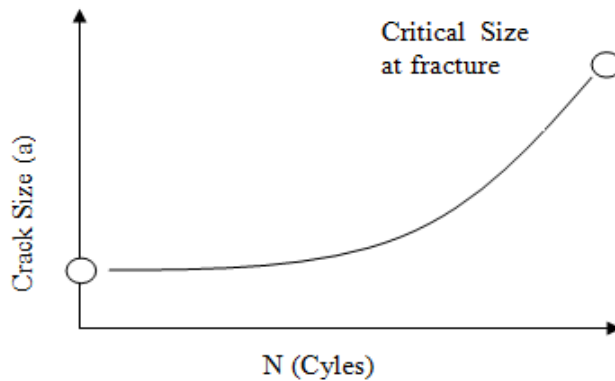


Figure 14 Schematic of fatigue crack growth (SAE, 1988, p.254).

For a single edge notch in mode I,

$Y(a) = 1,12$ for small cracks or

$$Y(a) = 1,12 - 0,231\left(\frac{a}{D}\right) + 10,55\left(\frac{a}{D}\right)^2 - 21,72\left(\frac{a}{D}\right)^3 + 30,39\left(\frac{a}{D}\right)^4 \quad (32)$$

up to $a/D = 0,6$

where

a = crack length,

D = width of the specimen

(Meyers & Chawla, 2009, p.426).

Assuming that $Y(a)$ varies as 1,12, 1,13, 1,14...to 1,41 for a continuous crack and a varies as 0,05, 0,06, 0,072...to 8mm with a constant ratio of 1,2, then from equation (29) and (30) the fatigue crack growth in geometric series starting at an initial crack size of 0,05 mm to a final crack length 8 mm is plotted against the number of stress cycles N as shown in Figure 15. Details of the inputs are given in Appendix 5.

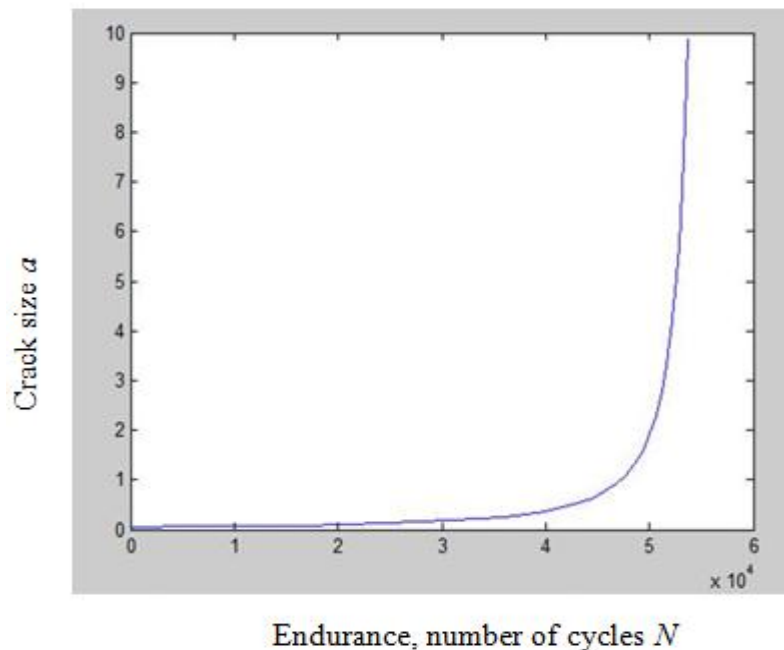


Figure 15 Fatigue crack growth.

From figure 15, as the number of stress cycles increases, the crack size widens until the critical size where fracture occurs. At the final crack size of 8mm, the fatigue life or the endurance ΔN is estimated to be 53646 cycles.

3.7 Brittle Fracture

Brittle fracture may occur with visibly, little or no plastic deformation and it is characterised by rapid crack growth (Liu, 2005). This means that once a crack sets in any part of the beam, the growth rate of the crack can be more spontaneous. This kind of fracture is rapid and it shows no necking (Liu, 2005). Macroscopic behaviour of brittle fracture is emphatically, more elastic up to the point of failure (Liu, 2005). Cracks can initiate in multiples at the same zone or different locations. Assuming a simple crack, the stress intensity factor is given by

$$K = \sigma \sqrt{\pi a} Y(a) \quad (33)$$

(Hobbacher, 2013, p.32).

Where

K = stress intensity factor depending on crack opening mode

σ = applied stress

a = half the crack length

According to Meyers & Chawla (2009), at a certain critical thickness, crack propagation is characterized by plane-strain conditions, where the stress intensity factor K_I in mode I case reaches a minimum value which is denoted as K_{IC} . The fracture mechanics can be used to predict life of crack from the onset to the critical size (SAE, 1988).

Four conditions that can lead to brittle fracture (Gorenc, Tinyou & Syam, 2012, p.30):

- loading at a temperature below the transition temperature of steel
- relatively high tensile stress, axial or bending
- presence of cracks, notches or triaxial stress states that lower the ductility of the detail
- use of steels having impaired ductility at the lowest service temperature.

4 COMPARISON WITH FEA RESULTS

Comparison of Load-Deformation Behaviour.

Laamanen (2013) carried out Finite element analysis of a 4x4mm plate and 8x8mm plate with plate element and solid element methods on FEMAP. The plate of 4mm thickness can be compared with the web of the I-beam. The curves obtained by Laamanen (2013) seem to predict higher deformation values compared to that obtained with the designed load from the analytical studies. Figure 16 shows the result of tensile and lateral buckling analysis obtained by Laamanen.

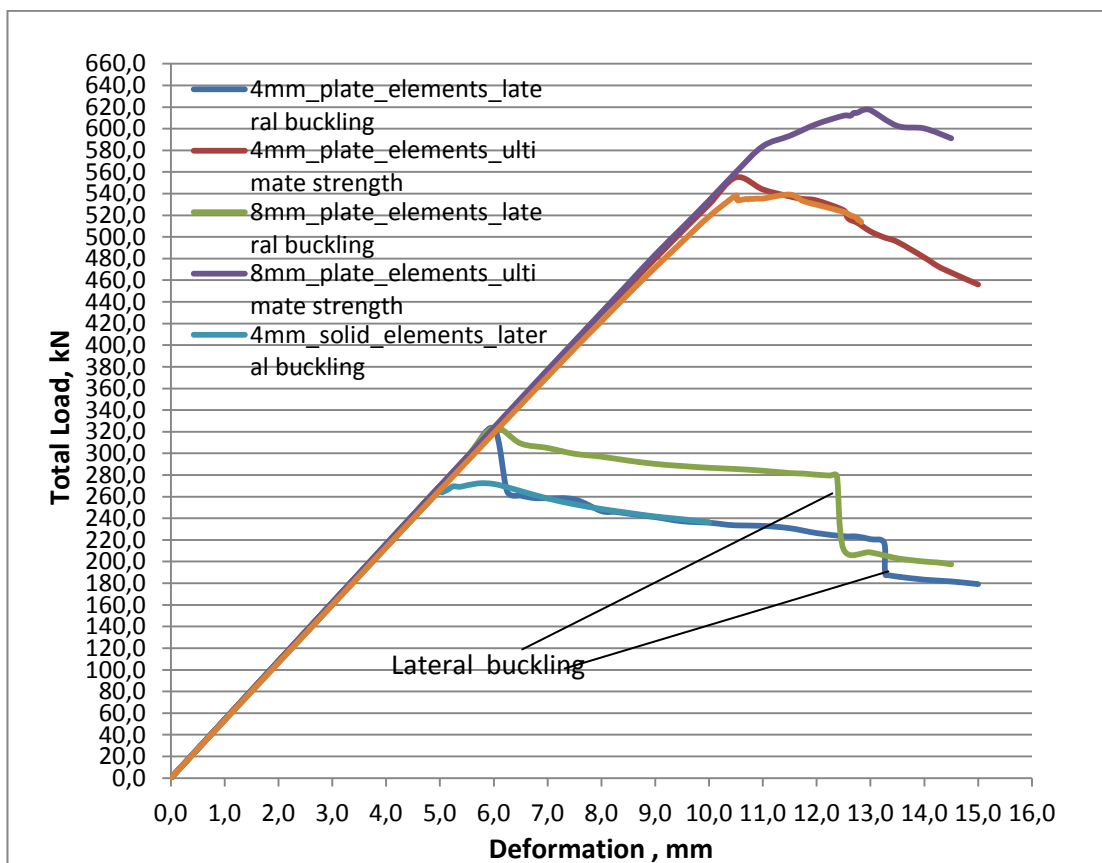


Figure 16 Load-deformation behaviour (Laamanen, 2013).

Comparison of Lateral Buckling Results.

From Laamanen's Load-deformation curve, evidence of lateral buckling is clearly seen. The plates seem to buckle laterally between 220 kN and 300 kN. Lateral buckling reduces the load carrying capacity of the plates by nearly half. The implication is that the initial design load of 600 kN will cause significant instability problem and perhaps ultimate failure of the I-beam.

In contrast, FEA predicted the maximum lateral buckling capacity $M_{b,Rd}$ to be 90 kNm whereas the analytical method gave 70,5-93,4 kNm. $M_{b,Rd}$ is a bit more than half the value of the designed moment M_{Ed} . The fact was that the maximum lateral buckling reduction factor was 0,54. The lower and upper bound moment capacities are due to the k_{ω} values. Table 9 shows the comparison of results of lateral buckling from both FEA and the analytical method.

Table 9 Comparison of lateral buckling analysis from FEA and analytical method.

	FEA results (Laamanen,2013)	Analytical Method results
Max. Loading capacity	300 kN	-
Lateral displacement	5,7 mm	-
Max. Stress	490-500 MPa	393-518 MPa
Max. Moment $M_{b,Rd}$	90 kNm	70,5-93 kNm

In both methods, the lateral buckling resistance moment $M_{b,Rd}$ is not adequate enough to satisfy the condition of safe design. The initial design bending moment M_{Ed} also exceeds the elastic moment capacity M_y . In other development, FEA was able to predict the lateral displacement whereas the analytical method could only predict the vertical displacement in static situations. The reason is that LTB behaviour in the analytical method was based on the material's geometric and elastic properties but visual lateral movement can be accessed experimentally. FEA could simulate to determine the lateral displacement when the load is applied. Experimentally, the lateral displacement could be measured after the application of the load.

Comparison of Static Analysis

The results of ideal case in FEA compare well with the analytical method. The slight discrepancy in deformation value may be as a result of boundary settings on the FEMAP or better resolution from FEA. Table 10 shows the comparison of results of the ideal case from both FEA and the analytical method.

Table 10 Comparison of static analysis from FEA and analytical method.

	FEA results (Laamanen,2013)	Analytical Method results
Max. Loading capacity	600 kN	600 kN
Max. Deformation	12,5 mm	9,4 mm
Max. Stress	960-970 MPa	998,7 MPa
Max. Moment M_{Ed}	180 kNm	180 kNm

The results from Table 10 are within the same range of accuracy. It can be argued that both methods predicted the maximum stress above the yield strength of the I-beam. Deformation values differ by 3,1 mm.

5 CONCLUSIONS

The capacity of the I-beam made of S960 QC has been investigated by following Eurocode 3. The objective of the thesis has been achieved and the following conclusions have been made after a comparative study of both analytical method and FEA results.

1. The elastic moment capacity $M_y = 172$ kNm and the plastic moment capacity $M_p = 198$ kNm. The slenderness of the I-beam implies that the plastic moment capacity is not large. The beam may fail shortly after exceeding the elastic capacity.
2. The initial designed load has to be lowered since the condition $M_{Ed}/M_{b,Rd} \leq 1$ has not been met. The maximum lateral buckling capacity $M_{b,Rd}$ obtained by FEA and analytical method is in a range of 90-93 kNm. The best alternative to improving safety of the I-beam would mean to reduce the initial designed load by half. That means each concentrated load will now be 150 kN and the corresponding bending moment M_{Ed} would be 90 kNm in order to satisfy the above condition.
3. The elastic critical moment which influences the lateral buckling capacity was found between 139,8-221 kNm. To ensure adequate stability the slenderness ratio of the beam has to be improved by altering the cross section width or thickness. Lower values of non-dimensional slenderness correspond to higher values of lateral buckling resistance factor. Higher reduction in lateral buckling will increase stability and load carrying capacity of the beam.
4. Lateral buckling reduction factor was between 0,41 and 0,54. This means that buckling could reduce the ultimate capacity nearly by half on the average. Warping capacity must be increased and adequate stiffeners must be provided against lateral-torsional buckling.

5. Buckling mode was purely lateral-torsional buckling. Local buckling was not evident.
6. The throat thickness was found to be 1,0 mm therefore the minimum requirement of 3mm must be used.
7. FEA predicted higher deformation values at ultimate loads than the analytical method. The difference is attributed to the boundary condition settings on FEMAP or mesh quality. Fine mesh sizes on FEMAP can increase the resolution and better deformation capacities are obtained which may be higher than the calculated value.
8. Fatigue life due to bending stress was found to be 65536 cycles by strength-life correlation. Fatigue assessment by crack propagation equation predicted the total fatigue life to be 53646 cycles based on nominal hot spot stress.

REFERENCES

Rautaruukki Corporation, Products & Solutions, *Optim QC ultra-high strength steels*, [online document]. [Accessed 10.07.2013]. Available at <http://www.ruukki.com/Product-s-and-solutions/Steel-products/Hot-rolled-steels/Structural-steels>

SFS EN 10025-6:2004+A1:2009 (E), p. 18.

Avery, P. , Mahendran, M., Nasir, A. (2000), *Flexural capacity of hollow flange beams*, Physical Infrastructure Centre, Journal of Constructional Steel Research 53 (2000) 201–223, Elsevier. [online document]. [Accessed 15.02.2013]. Available at <http://www.sciencedirect.com/science/article/pii/S0143974X9900067X>

Kim Y. Y., Kim, T. S. (2000), *Topology optimization of beam cross sections*. International Journal of Solids and Structures 37 (2000) 477±493, PERGAMON, Elsevier, [online document]. [Accessed 15.02.2013]. Available at <http://www.sciencedirect.com/science/article/pii/S0020768399000153#>

Juhás, P. (2009), *Challenges, Opportunities and Solutions in Structural Engineering and Construction, Elastic-Plastic bending load-carrying capacity of steels*, Edited by Nader Ghafoori, Chapter 22, ISBN 978-0-415-56809-8. [online document]. [Accessed 02.06.2013]. Available at <http://www.crcnetbase.com/doi/abs/10.1201/9780203859926.ch22>

Laamanen, T. (2013), Lappeenranta University of Technology, *I-beam profile and FEA results*.

Hämäläinen, O.-P. (2013) Master's Thesis, Lappeenranta University of Technology.

Björk, T., Toivonen, J., Nykänen, T. (2010), LUT, *Capacity of fillet welded joints made of ultra high strength steel*. Copyright © Rautaruukki Corporation. [online document]. [Accessed 18.05.2013]. Available at <http://www.ruukki.com/~media/Files/Steel-products/Technical-articles/Ruukki-Technical-article-Capacity-of-fillet-welded-joints-made-of-ultra-high-strength-steel.ashx>

Halme, T., Huusko, L., Marquis, G. (2010), Local buckling of plates made of high strength steel, Copyright © Rautaruukki Corporation, [online document]. [Accessed 18.05.2013] Available at <http://www.ruukki.com/~media/Files/Steel->

products/Technical-articles/Ruukki-Technical-article-Local-buckling-of-plates-made-of-high-strength-steel.ashx

International Association for Steel and Structural Engineering, IABSE (2005), *Use and Application of High-Performance Steels for Steel Structures*, pp.100-103, ISBN 3-85748-113-7, published by IABSE-AIPC-IVBH.

Hemmilä, M., Hirvi, A., Kömi, J., Laitinen, R., and others (2010), *Technological properties of direct-quenched structural steels with yield strengths 900 –960 MPa as cut lengths and hollow sections*, Ruukki Metals, Copyright © Rautaruukki Oyj, Finland. [online document]. [Accessed 18.05.2013]. Available at <http://www.ruukki.com/~/media/Files/Steel-products/Technical-articles/Ruukki-Technical-article-Technological-properties-of-direct-quenched-structural-steels.ashx>

SSAB Technology AB, Weldox High strength Steels, *Typical hardness of S960*. [online document]. [Accessed 25.05.2013]. Available at <http://www.ssab.com/en/Brands/Weldox/Products/Weldox-960/>

Kalpakjian, S., Schmid, Steven R. (2006), *Manufacturing Engineering and Technology*, 5th Edition, “*Ferrous Metals and Alloy*”, pp.128-133,149, 114, 960-961, Copyright by Pearson Education, Inc., 2006, U.S.A.

Kalpakjian, S., Schmid Steven R. (2008) *Manufacturing Processes for Engineering Materials*, copyright by Pearson Education, Inc., U.S.A.

Eurocode 3: European Standards: SFS EN 1993-1-1:2005, SFS EN 1993-1-5:2006, SFS EN 1993-1-8:2005, SFS EN 1993-1-9:2005.

Wang, Y.C. (2002), *Steel and Composite Structures, Behaviour and Design of Fire Safety, Local buckling of steel plates, Lateral torsional buckling*, pp.10-13.

Published by Spon Press, USA and Canada. ISBN 0-203-30224-9 Master e-book ISBN, ISBN 0-415-24436-6 (Printed Edition).

Hibbeler, R.C. (2005) *Moment of Inertia*, *Mechanics of Materials*, 2nd Edition, Published by Prentice Hall, Singapore. ISBN 0-13-186-638-9.

Egor, P. (1998), Engineering Mechanics of Solids, Second Edition, *Section modulus*, p. 339, ISBN 0-13-726159-4, Printed by Printice Hall, Inc., New Jersey, USA.

Gorenc, B. E, Tinyou, R., Syam, A. (2005), Steel Designers' Handbook, Seventh Edition, *Plastic Section Modulus*, p.223, 267, ISBN 0 86840 5736, Published by University of New South Wales Press Ltd, Sydney, Australia.

Delhi.edu, Lecture Material pdf, *Plastic Section Modulus*, [online document]. [Accessed 05.04.2013]. Available at: <http://faculty.delhi.edu/hultendc/AECT460-Lecture%206-F2009.pdf>

Hoogenboom, P.C.J. (2006), Warping stiffness, chap7 pdf, [online document]. [Accessed 20.03.2013]. Available at http://homepage.tudelft.nl/p3r3s/CT5141_chap7.pdf

Björk, Professor T. (2013), Lappeenranta University of Technology, *Instruction materials on warping constant and fatigue assessment*.

Punmia, B. C., Ashok, K. J, Arun, K, J. (2002), Mechanics of Materials, *Elastic Limit*, p.13, Available on google books.

David, W.A. R., (2006), Basic Engineering Plasticity, An Introduction and Manufacturing Applications, *Full elasticity*, p.128. ISBN-13: 978-0-7506-8025-7, Published by Elsevier Ltd.

Ferdinand, L. S., Andrew, P. (1980), Strength of Materials, Third Edition, *Deflection and Slope*, pp 271-273, ISBN 0-06-046229-9, Published by Harper & Row publishers, Inc., New York.

American Wood Council (2005) *Beam Formulas with Shear and Moment Diagrams*, Copyright by American Forest & Paper Association, Inc.,(2007). [online document]. [Accessed 03.06.2013]. Available at <http://www.awc.org/pdf/DA6-BeamFormulas.pdf>

Gorenc, B. E, Tinyou R., Syam, A. (2005), Steel Designers' Handbook, Seventh Edition, *Plastic Analysis, Plasticity*, p.266-268, ISBN 0 86840 5736, Published by University of New South Wales Press Ltd, Sydney, Australia.

Wang, Y.C. (2002), Steel and Composite Structures, *Behaviour and Design of Fire Safety, Local buckling of steel plates, Lateral torsional buckling*, pp.10-13.

Published by Spon Press, USA and Canada. ISBN 0-203-30224-9 Master e-book ISBN, ISBN 0-415-24436-6 (Printed Edition).

Wright H., *Stability and Ductility of Steel Structures*: Dubina Dan and Ivanyi Miklos (Eds); Elsevier, 1999, 620 pp. ISBN 0-08-043016-3., Engineering Structures, Volume 22, Issue 11, November 2000, Pages 1578-1579, ISSN 01410296, 10.1016/S0141-0296(00)00012-2.

Institute for Steel Development and Growth (INSDAG), Unrestrained Beam Design-I, version II, *Factors affecting lateral stability*, pp.11 21, [online document]. [Accessed 05.07.2013]. Available at <http://www.steel-insdag.org/TeachingMaterial/Chapter11.pdf>

Punmia, B. C., Ashok, K. J, Arun, K, J. (1998), Comprehensive Design of Steel Structures, *Lateral buckling of unrestrained I-beam*, p. 243, Available on google books.

Lehtinen, I. (2005), *Hitsatut profiilit, Käsikirja*, Ruukki, p.50-55, ISBN 952-9683-31-6.

Williams, A. (2001), Structural Steel Design, Volume 1: ASD, Plastic moment of resistance, pp. 97-98, ISBN 1-58001-055-5. Copyright by ICBO, Printed in U.S.A.

Adluri, Dr S., Memorial University, Canada, Lecture pdf. *Structural Steel Design Flexural Members, Bending pdf, Model of Behaviour*.

Ioannis G. R., Theodore A. (2010), *Critical Lateral-Torsional Buckling Moments of Steel Web-Tapered I-beams*, The Open Construction and Building Technology Journal, 2010, 4, 105-112. [online document]. [Accessed 01.04.2014]. Available at <http://www.benthamscience.com/open/tobctj/articles/V004/105TOBCTJ.pdf>

Maddox, S.J. (2002), *Fatigue strength of welded structures*, Second Edition, pp.1-22 Published by Abington Publishing, Woodhead Publishing Limited, England. ISBN 1 85573 013 8.

Radaj, D. (1990), Design and Analysis of Fatigue Resistant Welded Structures, *Fatigue strength dependent on number of cycles*, pp.66-89, ISBN 1 85573 004 9,

Liu, A. F. (2005), Mechanics and Mechanisms of Fracture, An Introduction, *Brittle fracture*, p. 66, ISBN 0-87170-802-7, Copyright by ASM International, printed in USA.

Pook, L. P. (2007), Metal Fatigue, What it is, why it Matters, pp.99-115, ISBN 978-1-4020-5596-6 (HB), ISBN 978-1-40205597-3, Published by Springer, Netherlands.

Hobbacher, A. (2013), International Institute of Welding (IIW), *Recommendations for Fatigue Design of Welded Joints and Components*, Feb. 2013 document, pdf.

Meyers, M., Chawla, K. (2009), Mechanical Behavior of Materials, Second Edition, *Crack propagation with elasticity*, pp. 171, 419-420, 737-739, ISBN 978-0-521-86675-0, Published by Cambridge University Press, New York, U.S.A.

SAE, (1988), Fatigue Design Handbook, AE-10, *Fatigue Crack Growth*, pp.253-255, ISBN 0-89883-011-7, Printed in U.S.A.

Gorenc, B. E, Tinyou, R., Syam, A. (2012), Steel Designers' Handbook, Eighth Edition, *Brittle fracture*, p.30, ISBN 9781742233413(pbk), 9781742245942(ePDF), Published by University of New South Wales Press Ltd, Sydney, Australia.

APPENDICES

Appendix 1 Stress distributions for effective width (1993-1-5:2006, p.17)

EN 1993-1-5: 2006 (E)

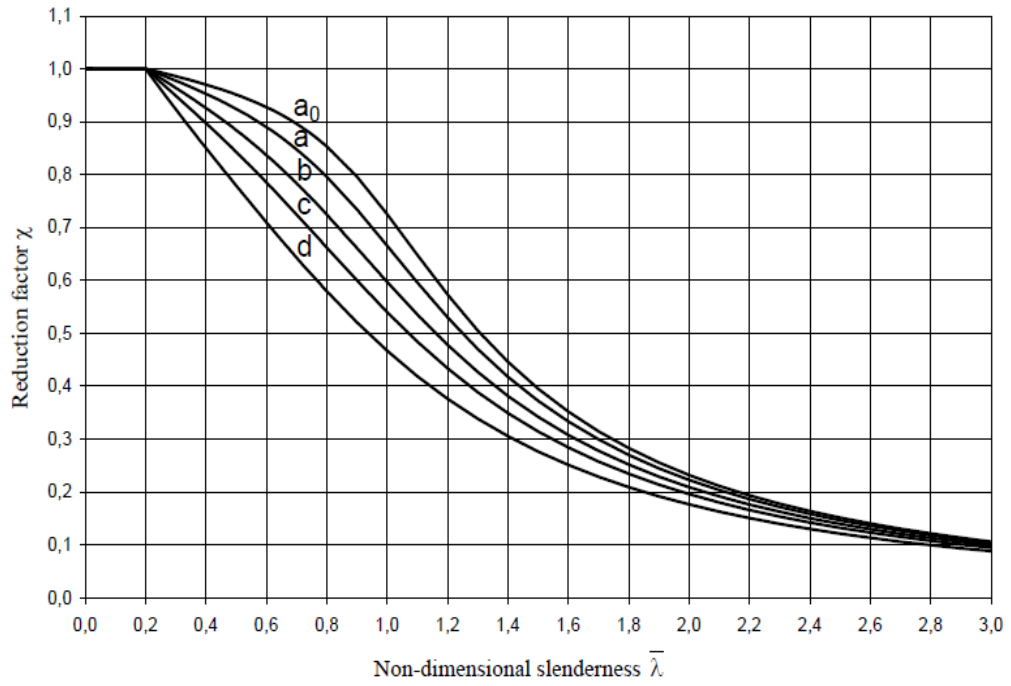
Table 4.1: Internal compression elements

Stress distribution (compression positive)				Effective ^p width b_{eff}		
				$\psi = 1:$ $b_{eff} = \rho \bar{b}$ $b_{e1} = 0,5 b_{eff} \quad b_{e2} = 0,5 b_{eff}$		
				$1 > \psi \geq 0:$ $b_{eff} = \rho \bar{b}$ $b_{e1} = \frac{2}{5 - \psi} b_{eff} \quad b_{e2} = b_{eff} - b_{e1}$		
				$\psi < 0:$ $b_{eff} = \rho b_c = \rho \bar{b} / (1 - \psi)$ $b_{e1} = 0,4 b_{eff} \quad b_{e2} = 0,6 b_{eff}$		
$\psi = \sigma_2 / \sigma_1$	1	$1 > \psi > 0$	0	$0 > \psi > -1$	-1	$-1 > \psi > -3$
Buckling factor k_σ	4,0	$8,2 / (1,05 + \psi)$	7,81	$7,81 - 6,29\psi + 9,78\psi^2$	23,9	$5,98 (1 - \psi)^2$

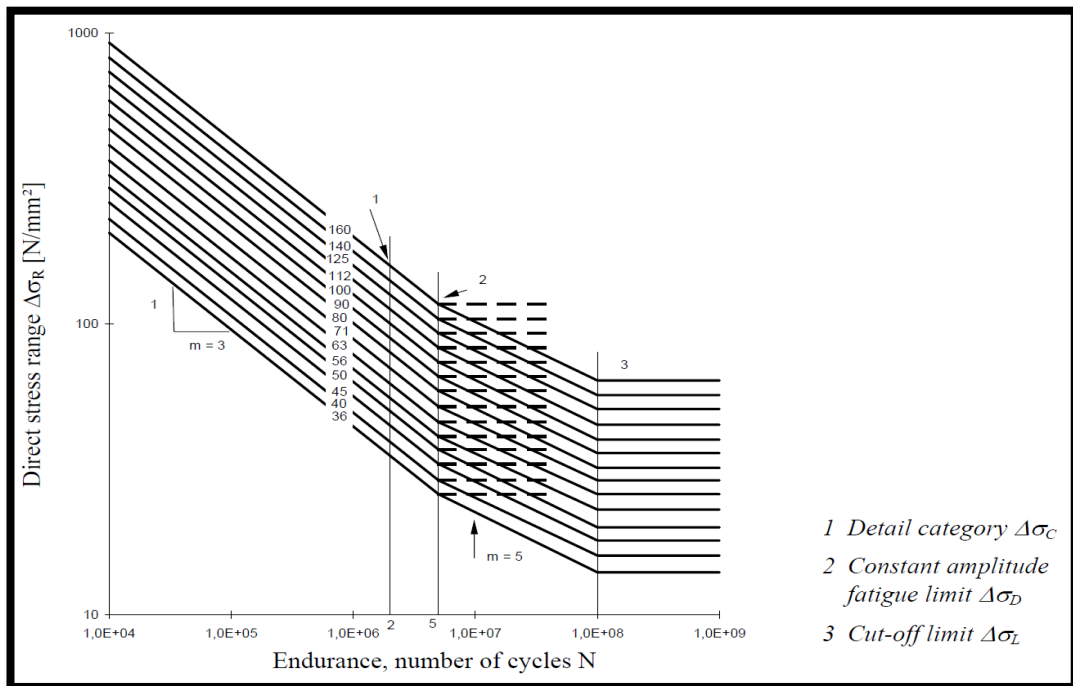
Table 4.2: Outstand compression elements

Stress distribution (compression positive)				Effective ^p width b_{eff}		
				$1 > \psi \geq 0:$ $b_{eff} = \rho c$		
				$\psi < 0:$ $b_{eff} = \rho b_c = \rho c / (1 - \psi)$		
$\psi = \sigma_2 / \sigma_1$	1	$1 > \psi > 0$	0	-1	$1 \geq \psi \geq -3$	
Buckling factor k_σ	0,43	0,57	0,85	$0,57 - 0,21\psi + 0,07\psi^2$		
				$1 > \psi \geq 0:$ $b_{eff} = \rho c$		
				$\psi < 0:$ $b_{eff} = \rho b_c = \rho c / (1 - \psi)$		
$\psi = \sigma_2 / \sigma_1$	1	$1 > \psi > 0$	0	$0 > \psi > -1$	-1	
Buckling factor k_σ	0,43	$0,578 / (\psi + 0,34)$	1,70	$1,7 - 5\psi + 17,1\psi^2$		

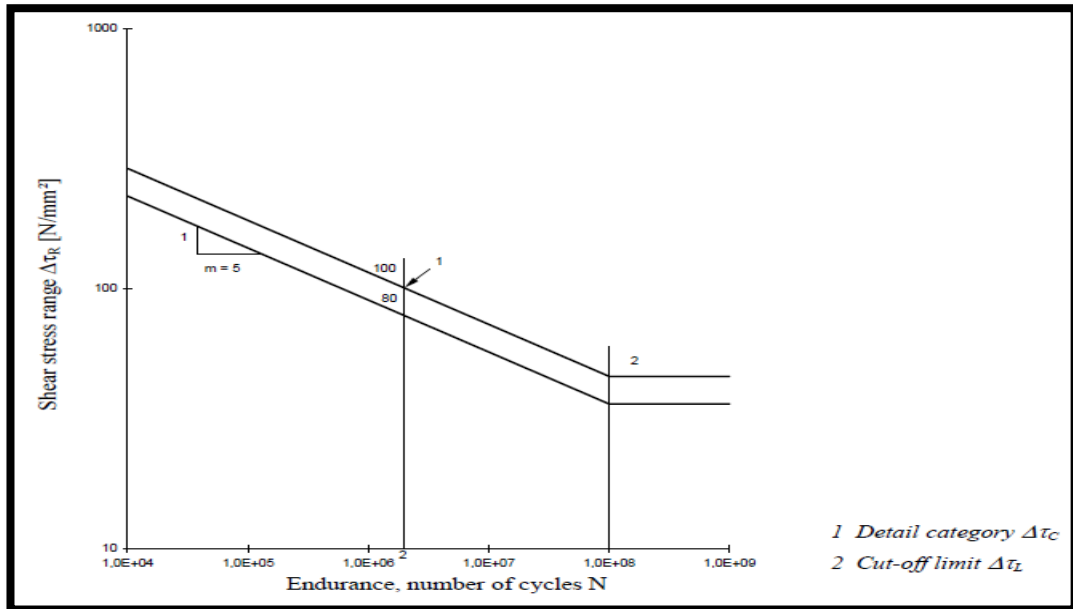
Appendix 2 Buckling curves (SFS EN 1993-1-1:2005(E), p.59)



Appendix 3 Fatigue strength curves for direct stress ranges (EN 1993-1-9: 2005(E), p. 15)



Appendix 4 Fatigue strength curves for shear stress ranges (EN 1993-1-9: 2005(E), p. 16)



Appendix 5 Inputs and function for fatigue life calculation based on Paris equation

$$\Delta\sigma_{h,spot} = \frac{\Delta\sigma_{nom}}{FAT} \cdot 100 = \frac{250 \cdot 100}{71} = 352 \text{ MPa}$$

```
function [N] = charles()

a_init = 0.05;
a_ratio = 1.2;

N_init = 0;

m = 3;
Mk = 1.02;
c = 3e-13;
Y_init = 1.12;
Y_diff = 0.01;
delta = 352;

steps = 30;
N = zeros(steps,1);
a = zeros(steps,1);
N(1) = N_init;
a(1) = a_init;
for i = 2:steps
    a(i) = a_init*a_ratio^(i-1);
    diff_a = a(i)-a_init*a_ratio^(i-2);
    diff_K = delta*Mk*(Y_init+(i-1)*Y_diff)*sqrt(pi*a(i));
    diff = c* diff_K^m;
    diff_N = diff_a/diff;
    N(i) = N(i-1)+diff_N;
end
plot(a,N);
```

ans =

$\Delta N = 53\ 646$ cycles.